DETERMINING A DIRECTION- AND POSITION-AGNOSTIC OCCUPANCY PROBABILITY AND OCCUPANCY RATIO FROM MAPS OF OBSTACLE FIELDS FOR GROUND VEHICLE NAVIGATION

Stephen J. Harnett, PhD Candidate[1,2], Sean Brennan, PhD[1], Karl Reichard, PhD[1,2], Jesse Pentzer, PhD[2]

[1]The Pennsylvania State University, University Park, PA
[2]The Applied Research Laboratory, The Pennsylvania State University, University Park, PA

ABSTRACT

Robot path-planning is a central task for navigation and most path-planners perform well in mapped environments with explicit obstacle boundaries. However, many obstacle fields are better defined by the probability of obstacles and obstacle geometries rather than by explicit locations. Few tools and data structures exist, other than repeated simulations, to predict robot mobility in these situations. Previously, it was shown that geometric obstacle properties could be used to estimate properties of paths routing around these obstacles, looking only at maps and avoiding the task of path planning [1]. This required knowing obstacle geometries relative to travel direction. This work presents a method for representing obstacle geometry, at arbitrary orientations and positions, and therefore a probabilistic model for determining if space near an obstacle is occupied. This paper explains the theory behind this method, uses this method to calculate the portion of a straight path overlapped by obstacles, called linear occupancy ratio, from simulated obstacle fields, and compares these results to measured occupancy ratio values to validate the probabilistic model.

1. INTRODUCTION

In the field of ground robotics, maps of obstacle fields can be used to solve for paths that keep the vehicle out of obstacles or reduce its time spent traversing obstacles, but if the mission is not known, it may be difficult to estimate path properties. There

are several well-known ways to represent noise or uncertainty in a mapped environment [2–5]. In addition to modeling noise, these methods can also be used to model untracked objects or objects that have not been recently tracked and whose states may have changed [6]. Additionally, many methods exist to semantically classify or track objects, despite the presence of uncertainty [7–9]. However, many of the resulting maps still require some mission knowledge, e.g. start and goal locations relative to the mapped obstacles, to plan a path from which to analyze path properties such as linear occupancy ratio. This work will show that linear occupancy ratio can be estimated without planning a path and therefore without knowing specific mission information such as start and goal locations.

Methods exist to build statistical likelihood maps based on observations [10, 11]. These techniques are not mutually exclusive with the data structure presented in this paper, rather, they could be used to build maps that are then stored as the occupancy probability functions presented here.

Previously, an experimental relationship was shown between map properties, such as obstacle size and density, and path properties [12]. This relationship can also be approximated without experiments, using only map properties [1]. The key contribution of this paper is a method for determining the probability of occupation for a mapped obstacle field without knowing the path or mission and therefore without knowing the vehicle position or orientation relative to the obstacles. This can be used in mission planning to describe the portion of a straight path through an environment that would require obstacle traversal.

The remainder of this paper is organized as follows: section 2 describes the way maps and paths will be measured and represented in this work, section 3 details the ways that obstacle geometry

and position can be probabilistically represented, section 4 utilizes these geometry and position representations to estimate a map property, linear occupancy ratio, and compares the result to measured data from simulation, and section 5 discusses applications of this method and areas for future work.

2. MAP AND PATH CHARACTERIZATION

In the remainder of this work, maps refer to 2D planes of free space populated by regions of occupied space representing traversable obstacles. Obstacles in the field may be sparse such that a path through the environment would barely be impacted by them, or obstacles may nearly tessellate the free space, forcing paths through the environment to route around or through many occupied regions. Polytopes represent obstacles and are stored in vertex-representation (vrep) [13]. Convexity is enforced so that collision checking calculations are simplified because a line segment will never enter, exit, and reenter a convex polytope [13].

To describe the size and spacing of obstacles in a field, this work uses departure ratio, r_D, a dimensionless parameter based on the average maximum radius, $\bar{R}$, of all polytopes in the field and number of obstacles per unit area, ρ, defined in equation (1). Higher departure ratio implies greater density of obstacles and/or larger obstacles. As departure ratio approaches 1, the obstacle field is nearly fully occupied. As departure ratio approaches 0, the obstacle field is nearly empty.

$$r_D = \bar{R}\sqrt{\rho} \qquad (1)$$

3. OBSTACLE POSITION AND GEOMETRY REPRESENTATIONS

This work presents two different methods for representing obstacle geometry. These methods are used to estimate occupancy ratio, a metric of how much space is occupied in a given obstacle field. Linear occupancy ratio is equal to the portion of a

Determining a Direction- and Position-Agnostic Occupancy Probability and Occupancy Ratio from Maps of Obstacle Fields for Ground Vehicle Navigation, Harnett, et al.

Page 2 of 11

straight line of unit length overlapped by obstacles; this affects both the amount of obstacle traversal that would be required by a vehicle crossing through obstacles and the amount of detouring that would be required by a vehicle routing around obstacles and is therefore a useful map property for understanding path complexity. This is described visually in figure 1.
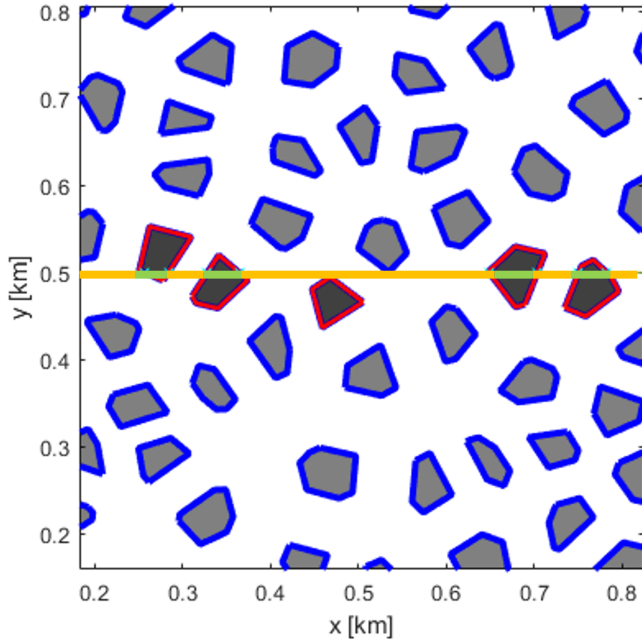

Figure 1: A straight line segment drawn through an obstacle field at an arbitrary location. The orange portions are in free space while the green portions are occupied by obstacles. Obstacles shown in red are those intersected by this line.

An obvious method to find linear occupancy ratio, $r_{L,occ}$, would be to take the square root of area occupancy ratio, $r_{A,occ}$, the portion of a unit square area occupied by obstacles, from some sampled area of the map. However, this approximation only holds for nearly square obstacles as shown in equations (2-5) which refer to dimensions, a, b, and c, defined in figure 2. The area occupancy ratio of a square field containing a square obstacle is as follows:

$$r_{A,occ,square} = \frac{(b-a)^2}{c^2} \qquad (2)$$

Therefore it is easy to see that the linear occupancy ratio of a square field containing a square obstacle, for a horizontal line passing through the center of the field, is equal to the square root of the expression shown in equation (2):

$$r_{L,occ,square} = \frac{(b-a)}{c} = \sqrt{r_{A,occ,square}} \qquad (3)$$

However, if a non-square obstacle in a square field is analyzed, in this case a right triangle, the area occupancy ratio becomes the following:

$$r_{A,occ,triangle} = \frac{\frac{1}{2}(b-a)^2}{c^2} \qquad (4)$$

The calculated linear occupancy ratio for this triangular obstacle, for a horizontal line passing through the center of the field, is then less than the square root of area occupancy ratio found in equation (4):

$$r_{L,occ,triangle} = \frac{\frac{1}{2}(b-a)}{c} < \sqrt{r_{A,occ,triangle}} \qquad (5)$$

Since it cannot be assumed that all fields and all obstacles are squares, taking the square root of area occupancy ratio should not be used to estimate linear occupancy ratio.

Determining a Direction- and Position-Agnostic Occupancy Probability and Occupancy Ratio from Maps of Obstacle Fields for Ground Vehicle Navigation, Harnett, et al.
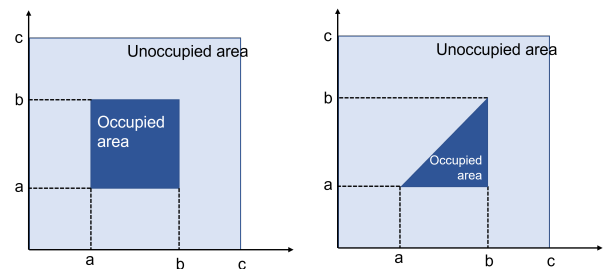
Page 3 of 11

Figure 2: Diagram of the dimensions used in equations (2-5) to show that the square root of area occupancy only equals linear occupancy for square obstacles in square fields.

To know the occupied or unoccupied length for a unit-length line, the occupied length per obstacle encounter and the number of obstacle encounters both need to be known. Prior work showed how to estimate the number of encounters accurately from ray casting [1]: lines are drawn through the mapped obstacle field and the number of obstacle intersections is tallied for each line and normalized by the length of the line. These lines are spaced apart by a decorrelation distance, related to obstacle size, so that neighboring lines are less likely to encounter the same series of obstacles. The number of intersections per unit length is then averaged for the set of lines drawn through the obstacle field to produce a single linear obstacle density number.

To determine the traversal distance required for each encounter, independent of obstacle orientation, the probability of space being occupied at a given radius from the centroid of the obstacle can be analyzed. This can be thought of as rotating the obstacle about its centroid to create a direction agnostic probability density function (PDF), an illustration of which is shown in figure 3. This work will discuss two ways to estimate occupied space per obstacle.
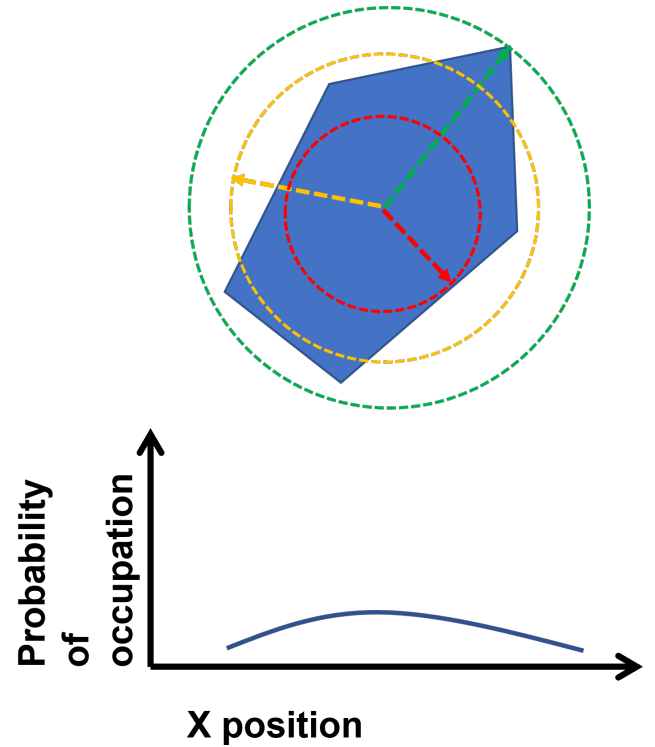

Figure 3: An illustration of an obstacle, rotated about its centroid, forming a radial probability density function where larger at larger radius values, shown in green, space is less likely to be occupied and at smaller radius values, shown in red, space is more likely to be occupied.

3.1. Inscribed Circle Estimate of Geometry

In this method, the size of an inscribed circle is estimated, as this is the region where the radial probability density function equals one, in other words, the radius at which the obstacle is always expected to occupy space regardless of the angular position. The estimated radius of an inscribed circle, $\hat{R}_{min}$, can be estimated using polytope vertex angle, θ_{vertex}, averaged over the entire field, and the distance from the centroid to the nearest vertex for each polytope, R_{min}, averaged over the entire field as shown in equation (6).

$$\hat{R}_{min} = sin(\frac{\bar{\theta}_{vertex}}{2}) \cdot \bar{R}_{min} \qquad (6)$$

Determining a Direction- and Position-Agnostic Occupancy Probability and Occupancy Ratio from Maps of Obstacle Fields for Ground Vehicle Navigation, Harnett, et al.

Page 4 of 11

Once the estimated size of the inscribed circle is known, the average traversal distance required to cross that circle must be found. This is the average width of the circular obstacle model, equal to the average value of a function representing the boundary of a circle. This is shown mathematically in equations (7-9) and visually in figure 4. The average value of function, $f(x)$, from input $x = a$ to input $x = b$ is:

$$f_{avg} = \frac{1}{b - a} \cdot \int_a^b f(x)dx. \tag{7}$$

Modifying equation (7) to give the average value of a function representing a circle with radius, r is then:

$$f_{circ,avg} = \frac{1}{r - (-r)} \cdot \int_{-r}^r \sqrt{r^2 - y^2}dy \tag{8}$$

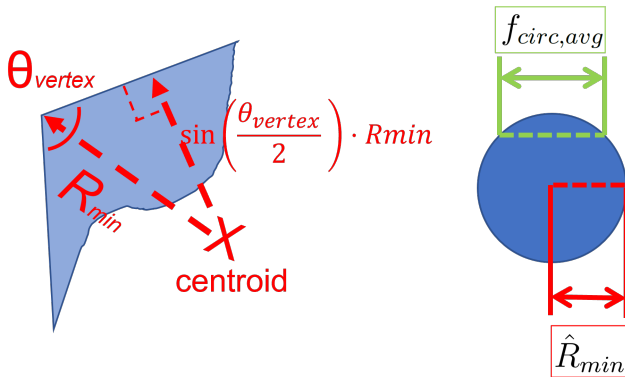$$= \frac{1}{2r} \cdot \frac{\pi r^2}{2} = \frac{\pi r}{4}. \tag{9}$$

Figure 4: A diagram of the parameters used in the method for estimating the size of the average inscribed circle and the average width of that circle. A polytope vertex is shown on the left and a circular obstacle model is shown on the right.

3.2. Radial Probability of Occupation to Represent Geometry

In this method, obstacles are represented by the radial PDF introduced earlier, describing the probability of space at some radius from the centroid

of the obstacle being occupied. The expected value of this PDF then informs an estimate of obstacle size.

First, equations for the polytope wall positions are converted from vertex representation in Cartesian coordinates to polar coordinates giving a function for radius as a function of angle from horizontal, $R(\theta)$. This is shown in figure 5.
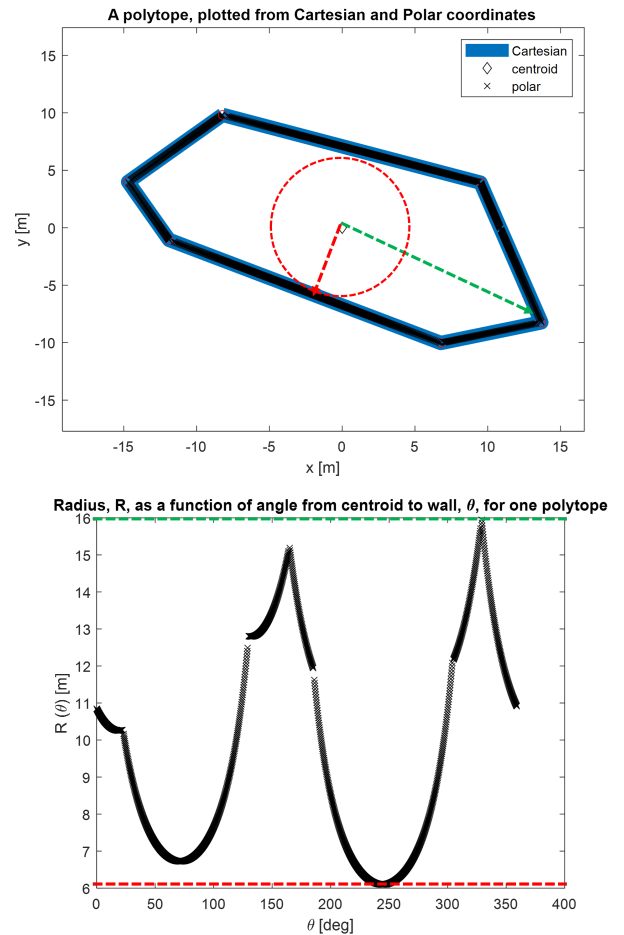

Figure 5: On the top is an example polytope, plotted in a Cartesian plane from both its rectangular and polar definitions. On the bottom is the polar function representing the same polytope. The minimum radius is shown in red on both plots and the maximum radius is shown in green.

Sampling this function at discrete angles, yields

Determining a Direction- and Position-Agnostic Occupancy Probability and Occupancy Ratio from Maps of Obstacle Fields for Ground Vehicle Navigation, Harnett, et al.

Page 5 of 11

a histogram, and therefore, from the law of averages, a probability density function (PDF) indicating the likelihood of a radius value, R, at any angular position, θ. From this, the complement of the cumulative density function (CDF) can be derived which is the probability of occupation, at some radius from the centroid. Once this function is known, the expected value of this function can be found to determine the expected width of an obstacle, independent of its orientation. This will be called the expected depth, d. For the polytope shown above, the PDF and complement of the CDF are shown in figure 6. The minimum radius for this polytope, below which the probability of occupation should be 1, is shown in red. The maximum radius for this polytope, above which the probability of occupation should be 0, is shown in green. The expected depth value, d, is shown in black. Notice the mean value of the minimum (6m) and maximum (16 m) is 11 m. The expected depth is less than this because the probability of occupation is higher at lower radius values, thus skewing the expectation lower.
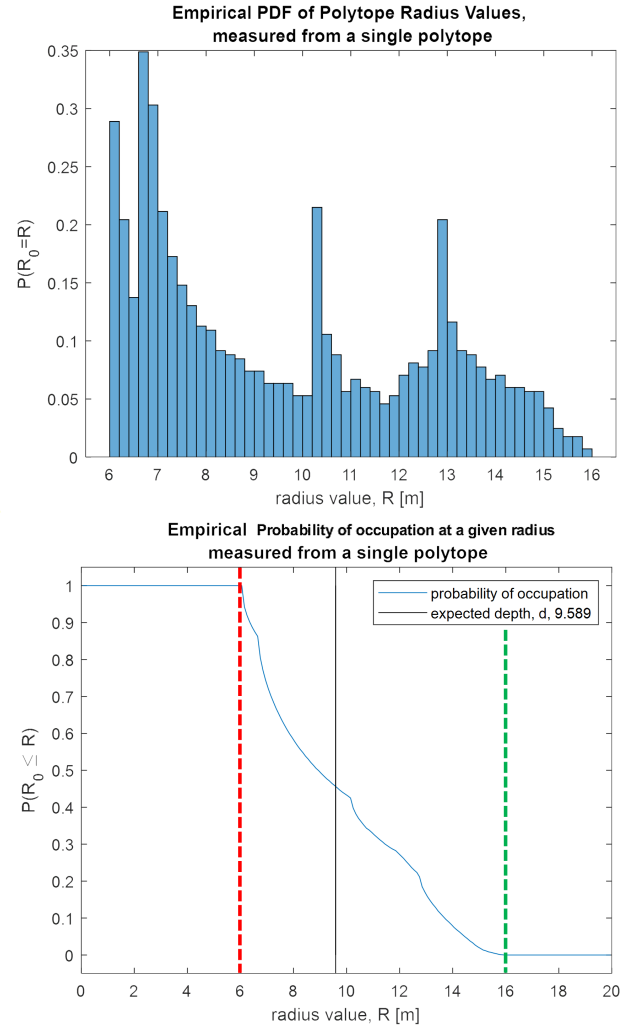

Figure 6: On the top is empirical PDF of polytope radii. On the bottom is the complement of the CDF, representing the probability of space being occupied at some radius.

The expected value, d, mentioned above is the radius of a circular obstacle model, calculated as shown in equation (10) using the complement of the CDF, $P(R_0 \leq R)$. A visual representation of this is shown in fig. 7. The probability of occupation will form a "bulls-eye" with the higher occupancy probability being concentrated at lower radii and the occupancy probability decreasing radially outward. This can be used to estimate the expected size of an encountered obstacle, independent of obstacle angle

Determining a Direction- and Position-Agnostic Occupancy Probability and Occupancy Ratio from Maps of Obstacle Fields for Ground Vehicle Navigation, Harnett, et al.

Page 6 of 11

relative to the direction of travel, but it is assuming that the obstacle is encountered along its centerline.

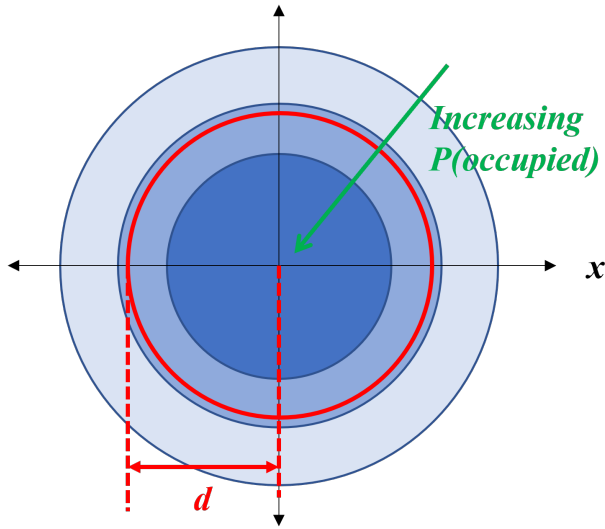$$d = \sum_{R=0}^{R_{max}} P(R_0 \le R) \cdot \Delta R \qquad (10)$$

Figure 7: A diagram of the radial probability of occupation, independent of angle from the centroid. The effective value of the radius, formed by a probability weighted sum of radii is shown as a red circle.

To find the expected obstacle size independent of both obstacle orientation and obstacle position relative to the direction of travel, another numeric integration is necessary. Integrating the probability of occupation, P, along a horizontal traversal line of length, $d(o)$, at different lateral positions offset from center, o, then yields effective depth at different offsets, d_{eff}, allowing for independence of position. This can be thought of as integrating the radial probability "bulls-eye" along the the line of variable length as a function of lateral offset, $d(o)$, rather than instead of along the axis going through the centroid of the "bulls-eye", where offset, 0, as was shown previously to find nominal expected depth, d. The relationship between the length of the line to integrate along, $d(o)$, and lateral offset is shown in

equation (11). The numeric integration is then shown in equation (12). A schematic of the parameters used in this process is shown in figure 8.

$$d(o) = \sqrt{R_{max}^2 - o^2} \qquad (11)$$

$$d_{eff} = \sum_{d=0}^{d(o)} P(R_0 \le \sqrt{o^2 + d^2}) \cdot \Delta d \qquad (12)$$
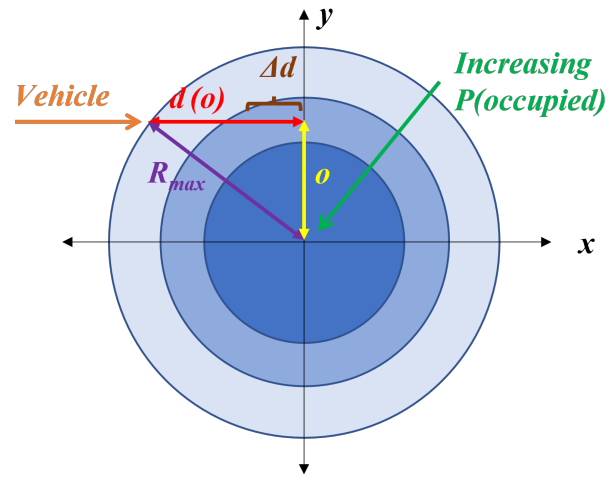

Figure 8: A schematic of parameters used in calculating expected depth as a function of lateral offset from the centroid of an obstacle. Lateral offset of the orange traversal vector is shown in yellow. The offset determines the length of the red line, along which the "bulls-eye" probability of occupation will be integrated numerically with step, Δd.

The effective depth as a function of offset can be plotted for every polytope in an obstacle field. The effective depth curve for a single polytope is expected to show that at an offset of 0, the effective depth is the expected value, d from Section 3.1. At an offset greater than or equal to the maximum radius, the effective depth approaches 0 as the lateral offset indicates the obstacle will not be encountered.

Analyzing this curve for all polytopes in a field shows they share a similar shape with different

Determining a Direction- and Position-Agnostic Occupancy Probability and Occupancy Ratio from Maps of Obstacle Fields for Ground Vehicle Navigation, Harnett, et al.

Page 7 of 11

scales. This is expected for a field of consistent obstacle aspect ratios. These curves can be averaged to give an expected effective depth curve independent of encountered polytope. The curves for all obstacles in an obstacle field and the average curve of these is shown in figure 9. Looking at the average value of the average curve gives an obstacle size estimate that is independent of both orientation and position.
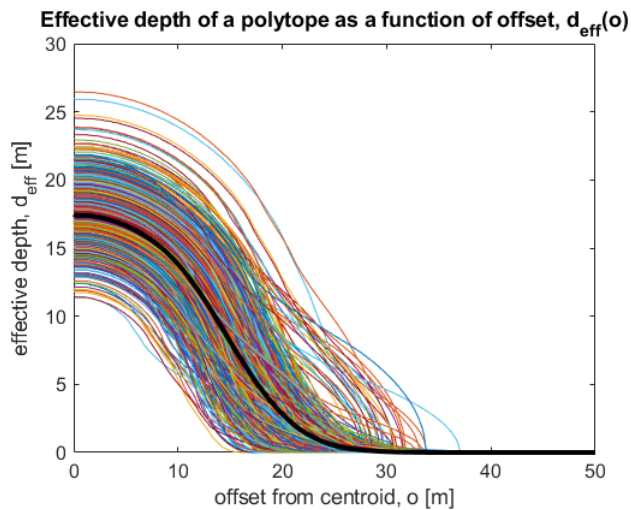

Figure 9: Effective depth as a function of offset position shown for every polytope in an obstacle field. The heavy black line is the average curve, representing the expected geometry independent of encountered obstacle.

4. RESULTS

Combining the statistical representations of obstacle size from Section 3 with the ray-casting-based estimate for the number of encountered obstacles [1], an estimate for linear occupancy ratio can be produced and compared to measured values from simulation. A comparison of these estimates and measured data is shown in figure 10.
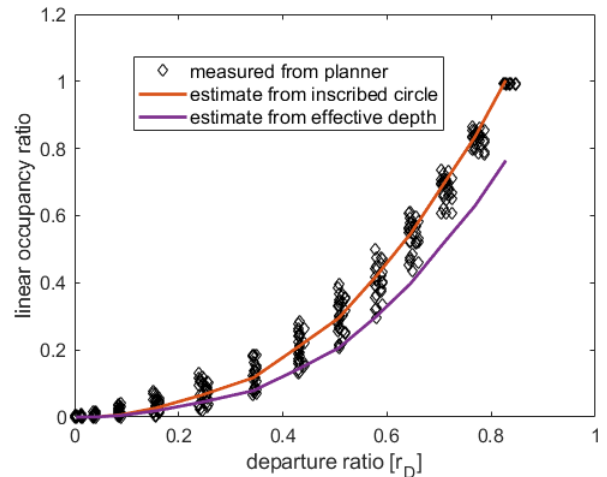

Figure 10: A comparison of linear occupancy ratio calculated using both probabilistic obstacle representations mentioned in Section 3 plotted with a scatter of measured occupancy ratios from simulated obstacle field maps. The orange curve is calculated from the inscribed circle method described in Section 3.1, and the purple curve is calculated from the radial probability of occupation as described in section 3.2.

It is worth noting that the radial probability of occupation method will provide a conservative estimate of obstacle size because the polytope size distribution is right skewed, as shown in figure 11, and therefore encounters with outliers of larger size may easily increase the measured values. This is because the floor of polytope size is zero while the ceiling approaches infinity. The more circular the polytopes in a field are, the less skewed the distribution of radii would appear. The expected value will be slightly less than the average value. The inscribed circle estimate works well for obstacles with approximately square aspect ratios, but is expected to not work well for more oblong obstacles, while the effective depth method is expected to be robust to oblong obstacles as it is based on an empirically sampled probability density function. Another observation to note from this testing is that the effective depth curves shown in figure 9 are very sensitive to the offset value selected, which is clear

Determining a Direction- and Position-Agnostic Occupancy Probability and Occupancy Ratio from Maps of Obstacle Fields for Ground Vehicle Navigation, Harnett, et al.

Page 8 of 11

from the steep slope of approximately -2 in the offset range from $10 - 20$ meters. The implications of this will be discussed further in the next section.
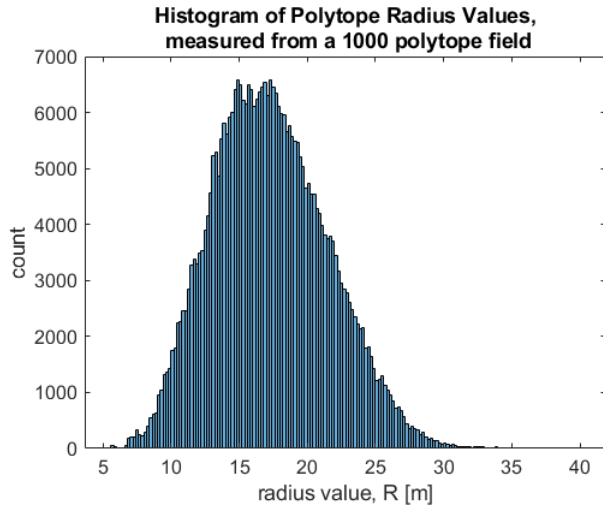

Figure 11: A histogram of polytope radius values, sampled at every degree from every polytope.

5 CONCLUSIONS

One application of this method would be compressing representations of obstacle field maps, where representing an entire field as "bulls-eyes" formed from radial occupancy probability, spaced apart by average obstacle density could be achieved. In this way, the entire field can be approximated by just the average effective depth curve from figure 9 and a scalar linear density value. This probabilistic representation could also be used to represent obstacles out of the field of view or in unmapped regions or seldom mapped regions, until better information is available to updated predictions. The effective depth curves developed in this work could also be extended to create a path planner that intelligently "apexes the turn" around obstacles to optimize travel speed, even for obstacles that cannot be seen, by allowing the planner to pass obstacles at a lateral offset value that has some acceptable probability of encountering occupied space without

having to conservatively route around obstacles based on their maximum possible size. This is powerful because it allows for planners to go beyond the binary through or around decision and solve for an optimal offset distance, at which the path planner should accept the risk of passing through the shape by "clipping the corner" and taking a straighter path while also minimizing time spent traversing obstacles.

Another way to apply radial probability of occupation to representing obstacles, is to capture uncertainty in object size rather than accounting for uncertainty of orientation. E.g. if a tree top is visible from an overhead satellite map, a map of radial probability functions could represent the likely trunk locations. This could allow a planner to attempt to route under the canopy while avoiding the tree trunks.

The limitations of this work include that simulated maps were generated by forming Voronoi cells [14] around the Halton point set, to generate pseudo-random yet evenly spaced obstacle locations [15]. In other words, the simulated polytope obstacle fields used in this work were likely to have evenly spaced obstacles with approximately square aspect ratios. Less uniformly spaced and uniformly sized obstacles may be less accurately approximated by this method. As mentioned in the previous section, the inscribed circle estimate assumes nearly circular obstacles and would not work well for non-square aspect ratios while the effective depth method is expected to still perform well so long as obstacles are still randomly oriented as it uses an empirically derived probability density function. However if obstacles had non-square aspect ratios and were not randomly oriented, i.e. if the aspect ratios of obstacles were aligned on some axis, then the empirically derived probability density function may not capture this as it is dependent only on radius. Thus, to apply this method to

Determining a Direction- and Position-Agnostic Occupancy Probability and Occupancy Ratio from Maps of Obstacle Fields for Ground Vehicle Navigation, Harnett, et al.

Page 9 of 11

non-square aspect ratios and non-randomly oriented obstacles it may be necessary to extend this method to higher dimensions, i.e. to have the probability density function depend on more than one variable. E.g. if obstacles are longer in the x-direction and smaller in the y-direction and are consistently oriented that way, it would make sense to form a higher dimensional expected depth function with probability of occupation as a function of x-position relative to obstacle centroid and probability of occupation as a function of y-position as a function of centroid. Thus the linear occupancy ratio estimate would be able to have a direction-dependence. This extension to higher dimensions is non-trivial and an area for future work.

As mentioned in the previous section, the effective depth curve changes dramatically for different offset values. This work assumed all offset values were equally likely to occur when selecting an expected offset and therefore an expected depth. Thus, it may be possible to develop a method to intelligently inform expected offset, based on expected obstacle density, as traversing a more densely populated field would require crossing more obstacles at low offset values, close to their centers, while traversing a more sparsely populated field would result in grazing more obstacles at larger offset values. Strategically selecting an offset value rather than assuming all offset values are equally likely to occur could improve the accuracy of this estimate.

In summary, this paper presented a method for representing obstacles of unknown position and orientation using the concept of a probability of occupation, spaced apart by an expected density. This allows for estimating properties such as linear occupancy ratio without knowing the path or mission and therefore without knowing the vehicle position or orientation relative to the obstacles. This work can be applied to abstract entire maps to a scalar number representing density and a function representing expected obstacle size as a function of lateral offset

of the traversal direction.

6. REFERENCES

[1] S J Harnett, S Brennan, K Reichard, J Pentzer, S A Tau, and D Gorsich. Path-free estimation of navigation distance using obstacle shape statistics and density. *Proceedings of the 2022 Ground Vehicle Systems Engineering and Technology Symposium (GVSETS)*, 2022.

[2] Rami Al-Hmouz, Tauseef Gulrez, and Adel Al-Jumaily. Probabilistic road maps with obstacle avoidance in cluttered dynamic environment. *Proceedings of the 2004 Intelligent Sensors, Sensor Networks and Information Processing Conference, ISSNIP '04*, pages 241–245, 2004.

[3] Lars Blackmore, Hui Li, and Brian Williams. A probabilistic approach to optimal robust path planning with obstacles. *Proceedings of the American Control Conference*, 2006:2831–2837, 2006.

[4] Kai M Wurm, Armin Hornung, Maren Bennewitz, Cyrill Stachniss, and Wolfram Burgard. Octomap: A probabilistic, flexible, and compact 3d map representation for robotic systems. *Proc. of the ICRA 2010 workshop on best practice in 3D perception and modeling for mobile manipulation*, 2, 2010.

[5] Jesse Levinson and Sebastian Thrun. Robust vehicle localization in urban environments using probabilistic maps. *Proceedings - IEEE International Conference on Robotics and Automation*, pages 4372–4378, 2010.

[6] Myungsoo Jun and Raffaello D'Andrea. Probability map building of uncertain dynamic environments with indistinguishable obstacles. *Proceedings of the American Control Conference*, 4:3417–3422, 2003.

Determining a Direction- and Position-Agnostic Occupancy Probability and Occupancy Ratio from Maps of Obstacle Fields for Ground Vehicle Navigation, Harnett, et al.

Page 10 of 11

[7] Sebastian Ramos, Stefan Gehrig, Peter Pinggera, Uwe Franke, and Carsten Rother. Detecting unexpected obstacles for self-driving cars: Fusing deep learning and geometric modeling. *IEEE Intelligent Vehicles Symposium, Proceedings*, pages 1025–1032, 7 2017.

[8] François Fleuret, Jérôme Berclaz, Richard Lengagne, and Pascal Fua. Multicamera people tracking with a probabilistic occupancy map. *IEEE Transactions on Pattern Analysis and Machine Intelligence*, 30:267–282, 2 2008.

[9] Timur Bagautdinov, François Fleuret, and Pascal Fua. Probability occupancy maps for occluded depth images. *Proceedings of the IEEE Conference on Computer Vision and Pattern Recognition (CVPR)*, pages 2829–2837, 2015.

[10] Sebastian Thrun, Jens-Steffen Gutmann, Dieter Fox, Wolfram Burgard, and Benjamin J Kuipers. Integrating topological and metric maps for mobile robot navigation: A statistical approach. *AAAI-98 Proceedings*, pages 989–995, 1998.

[11] Daniel Pagac, Eduardo M. Nebot, and Hugh Durrant-Whyte. Evidential approach to probabilistic map-building. *Proceedings - IEEE International Conference on Robotics and Automation*, 1:745–750, 1996.

[12] Seth Tau. The effects of path-planning uncertainty on intelligent vehicle performance, 2021.

[13] Branko Grünbaum. *Convex Polytopes*, volume 221. Springer New York, 2003.

[14] Mark De Berg, Otfried Cheong, Marc Van Kreveld, and Mark Overmars. *Computational geometry: Algorithms and applications*. 2008.

[15] J. H. Halton. Algorithm 247: Radical-inverse quasi-random point sequence. *Communications of the ACM*, 7, 1964.

Determining a Direction- and Position-Agnostic Occupancy Probability and Occupancy Ratio from Maps of Obstacle Fields for Ground Vehicle Navigation, Harnett, et al.

Page 11 of 11